

Tectonic consequences of Martian dichotomy modification by lower-crustal flow and erosion

Francis Nimmo Department of Earth Sciences, University of California–Santa Cruz, Santa Cruz, California 95064, USA

ABSTRACT

The Martian hemispheric dichotomy shows compressional features a few hundred kilometers south of the dichotomy boundary, and contemporaneous extensional features along the boundary. Two processes that may have contributed to the observed deformation are lateral lower-crustal flow and erosion. Crustal flow causes a decrease in crustal thickness in the south, and an increase in the north. The result is compressional surface stresses in the highlands and extensional stresses around the dichotomy boundary. The magnitude, location, and timing of the predicted stresses are consistent with the observed tectonic features and strongly suggest that moderate lateral flow occurred. For the nominal heat flux and rheology, sufficient lateral flow is generated for a mean crustal thickness of 70 km. Erosion generates extension in the south and compression in the north, opposite to what is observed. Either erosion only resulted in local, as opposed to regional, distribution of highland material, or the rigidity of the lithosphere was sufficiently high at the time of erosion that significant stresses did not develop.

Keywords: Mars, tectonics, rheology, stress, rigidity.

INTRODUCTION

Mars has systematically higher topography and thicker crust in its heavily cratered southern hemisphere (Zuber et al., 2000). The origin of this dichotomy is still uncertain (e.g., Frey and Schultz, 1988; McGill and Dimitriou, 1990; Zhong and Zuber, 2001). Here I focus on two mechanisms (lateral crustal flow and erosion) by which the dichotomy may have been modified subsequent to its development. Models of these mechanisms in comparison with observations of tectonic deformation provide constraints on conditions on early Mars, and potentially on the formation of the dichotomy.

Lateral crustal thickness variations, even if isostatically compensated, generate pressure gradients that can drive flow in the lower crust (e.g., Bird, 1991). On Mars, crustal flow models have been used to place an upper bound on the Martian crustal thickness of ~100 km (Zuber et al., 2000; Nimmo and Stevenson, 2001). However, little attention has hitherto been paid to the tectonic consequences of limited lateral crustal flow.

The degradation of craters in the southern highlands and the identification of numerous inliers suggest that significant amounts of erosion occurred during the late Noachian (e.g., Craddock and Maxwell, 1993; Hynes and Phillips, 2001). Estimates of the amount of material removed are ~1 km, although it is unclear what fraction of this material was re-deposited locally, as opposed to having been transported into the northern plains.

OBSERVATIONS

The specific area of the dichotomy examined in this paper is shown in Figure 1A. The high topography of the southern highlands is

evident, as is the Isidis impact basin. The lower northern plains contain another impact basin, Utopia, and the volcanic rise of Elysium. The margins of the highlands consist of Hesperian-age boundary plains, whereas the lowland surface material is late Hesperian–early Amazonian (Tanaka et al., 2003). The lowlands contain partially buried quasi-circular depressions, which have been inter-

preted as impact basins (Frey et al., 2002). The implied age of the lowland basement is early Noachian, and no more than ~100 m.y. younger than the dichotomy age of ca. 4.1 Ga (Frey, 2004).

Figure 1B shows two stacked topographic profiles across the area of interest. Both show two features, also visible in individual topographic profiles (e.g., Irwin et al., 2004): a relatively steep (1° – 2°) scarp, typically 100–200 km wide; and beyond it to the north a transition zone of comparable width that is higher than the background plains and is rough. The roughness is due to the presence of knobby material, possibly crater remnants (McGill et al., 2004; cf. Irwin et al., 2004). This transition zone contains the boundary plains materials of Tanaka et al. (2003).

The tectonics of this area of the dichotomy were investigated by McGill and Dimitriou (1990), Watters (2003b), and Tanaka et al. (2003), among others. Compressional features (lobate scarps) are found a few hundred kilometers south of the dichotomy boundary (Watters, 2003a, 2003b), whereas extensional features are concentrated within and below the

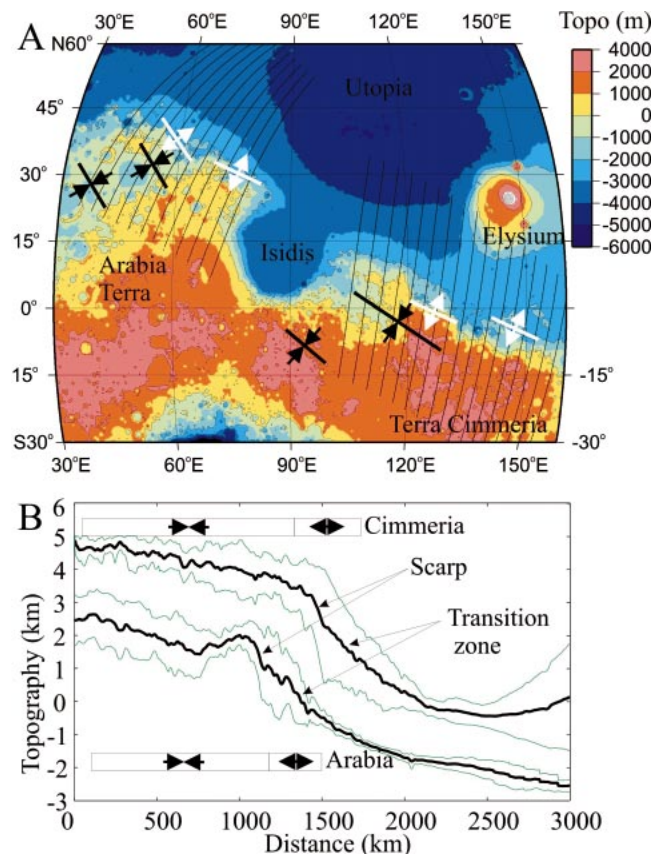


Figure 1. A: Mars topography from 0.25° gridded data obtained by Mars Orbiter Laser Altimeter, Robinson projection, centered at 95°E. Thin lines denote individual profiles used to generate Figure 1B. Black and white arrows denote areas of compression and tension, respectively, after Watters (2003a). **B:** Topographic profiles (bold lines), generated by stacking individual profiles to west (Arabia) and east (Cimmeria) of Isidis Basin. Cimmeria profile offset vertically by 2 km for clarity. Vertical exaggeration is 200:1. Thin lines denote \pm one standard deviation. Boxes with arrows denote approximate locations of compressional and extensional regions from A.

scarp (McGill and Dimitriou, 1990; McGill et al., 2004) (see Fig. 1B). The lobate scarps cut late Noachian and early Hesperian materials, suggesting that faulting was active during this period (see discussion in Watters and Robinson, 1999). McGill and Dimitriou (1990) and McGill et al. (2004) concluded that the extensional faulting could not have occurred earlier than the late and middle Noachian, respectively. Tanaka (2004) noted that reactivation of preexisting structures can result in underestimates for the age of deformation. Thus, although dichotomy formation preceded the development of the tectonic features, the absolute time interval between these two events is uncertain, but it probably exceeds 200 m.y.

Watters and Robinson (1999) estimated a strain of 0.17% associated with the lobate scarps. The strains associated with the normal faults in the vicinity of the dichotomy are ~3.5% (McGill et al., 2004), but some of this extension may be due to gravity-driven, shallow tectonics, similar to the development of the Canyonlands grabens of Utah (Schultz-Ela and Walsh, 2002). Overcoming friction on a dry fault ~10 km deep requires stresses of ~70 MPa.

The bulk of the southern highlands is close to isostatically compensated (elastic thickness, T_e of <16 km) (McGovern et al., 2002; McKenzie et al., 2002). However, the rigidity of the Martian lithosphere probably increased after the highlands formed. Isidis, Utopia, and Elysium show large positive gravity anomalies, indicative of substantial elastic strength (Zuber et al., 2000). Nimmo (2002) obtained larger T_e values (37–89 km), probably because of contamination from the more rigid northern lowlands. Watters (2003a) fitted dichotomy topographic profiles to obtain a T_e of 31–36 km.

MODEL

Figure 2 gives a conceptual outline of the two models to be employed. In each case, the initial topography is assumed to be isostatic. For the crustal flow model (Fig. 2A), lateral flow of lower crustal material results in a reduction in height of the thick-crust side, and vice versa. These deflections result in compression on the thick-crust side, and (primarily) extension on the thin-crust side. Conversely, if surface erosion occurs on the thick-crust side (Fig. 2B), the resulting unloading will generate uplift on the thick-crust side and vice versa. This uplift will generate extension on the thick-crust side and compression on the thin-crust side.

There are two approaches to modeling lower crustal flow. One assumes that all rheologies are Newtonian; the advantage of this approach is that it is relatively straightforward to incorporate elastic effects (e.g., Zhong, 1997; Zhong and Zuber, 2000). Alternatively, a more realistic non-Newtonian rheology may

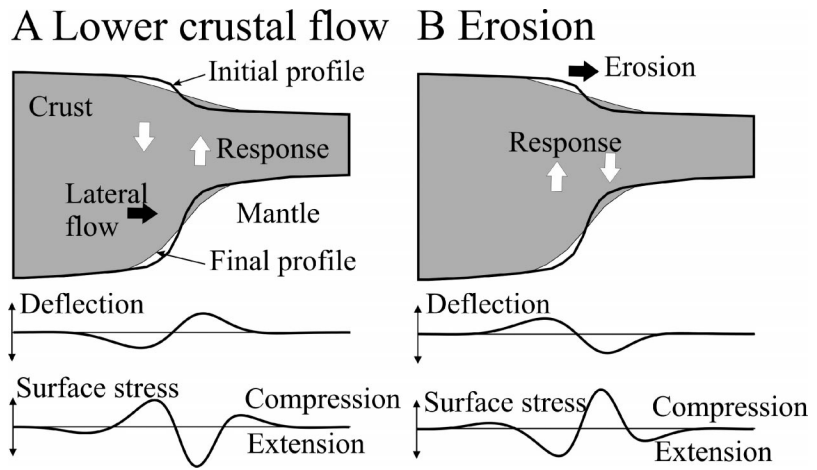


Figure 2. A: Conceptual model for stresses resulting from lower crustal flow. Lateral flow leads to uplift on thin-crust side, and vice versa. Stress is calculated from second derivative of deflection and results in compression on thick-crust side and (primarily) extension on thin-crust side. B: Similar model for stresses resulting from surface erosion. Removal of material on thick-crust side results in uplift. Resulting stresses are extensional on thick-crust side and (primarily) compressional on thin-crust side.

be assumed (e.g., Bird, 1991; Nimmo and Stevenson, 2001); the disadvantage is that incorporation of elastic effects then becomes much more difficult.

The approach employed here is described in detail in Nimmo and Stevenson (2001). The evolution of the crustal thickness is described by a diffusion-like differential equation, where the (spatially varying) diffusion coefficient depends on the crustal temperature structure and rheology. The temperature structure within the crust is determined by the decay of radioactive materials within and below the crust.

To account for the nonzero rigidity, and to allow calculation of elastic stresses, the deflection of the surface from its initial (isostatic) position is calculated as follows. The net redistribution of lower crustal material owing to lateral flow, calculated using the method just described, is converted into an effective load $L(x)$ using $L(x) = \Delta\rho gr(x)$, where $\Delta\rho$ is the density contrast between crust (density ρ_c) and mantle (ρ_m), g is acceleration owing to gravity, $r(x)$ is the change in crustal root thickness, and x is the horizontal coordinate. The surface deflection $w(x)$ in response to this load is given by (Turcotte and Schubert, 2002):

$$D \frac{d^4 w}{dx^4} + w \rho_c g = L(x), \quad (1)$$

where $D = ET_e^3/12(1 - \nu^2)$, E is Young's modulus, and ν is Poisson's ratio. In practice, this equation is most easily solved in the wave-number domain. The final topography is the initial (isostatic) topography minus w . The surface elastic stresses $\sigma(x)$ caused by this deflection w may then be calculated, using (Turcotte and Schubert, 2002):

$$\sigma(x) = \frac{E}{1 - \nu} \frac{T_e}{2} \frac{d^2 w}{dx^2}. \quad (2)$$

This approach reproduces the original isostatic topography in the limit as $T_e \rightarrow 0$. Furthermore, as long as the flexural parameter $\alpha = (4D/\rho_m g)^{1/4}$ is small in comparison to the distance over which lower crustal flow occurs, the use of the isostatic assumption in calculating the flow will not introduce significant errors. For a T_e of 30 km, $\alpha = 92$ km, which is significantly smaller than the dichotomy length scale. Thus, for the parameters of interest here, the method described is likely to be adequate.

PARAMETERS ADOPTED

For the nominal case, a mean crustal thickness of 70 km was assumed. The time-dependent heat flux was calculated by assuming initial mantle radiogenic concentrations given by Wanke and Dreibus (1988). The resulting initial values for depleted mantle heat flux and crustal heat generation were 65.8 mWm^{-2} and 0.055 μWm^{-3} , respectively. These values had decreased by 4.6% by the end of the 100 m.y. model run. The crustal rheology adopted was dry diabase (Mackwell et al., 1998), the crust and mantle densities were 2900 kg m^{-3} and 3400 kg m^{-3} , respectively, and Young's modulus was 100 GPa. The time step was 10^{10} s, and the grid spacing 10 km; other parameters were kept the same as the nominal values in Nimmo and Stevenson (2001).

RESULTS

Figure 3A shows the evolution of the topography of the base of the crust as a function of time, calculated using the method previ-

ously described. Most of the crustal flow happens early, because this is the time at which stresses and the temperature at the base of the crust are highest. After 100 m.y., flow has effectively ceased. The dashed line shows the local change in depth to the base of the crust at the end of 100 m.y. It is this redistribution of crustal material that generates a load on the near surface, and that allows the resulting deflection to be calculated (equation 1).

Figure 3B shows the topography that results from this crustal redistribution, calculated for three values of the elastic thickness T_e . The initial profile is given by the dotted line. For large elastic thicknesses, the final profile closely resembles the initial profile, because the deflection of the lithosphere is small. Conversely, for small elastic thicknesses, the topographic profile is close to a mirror image of the crustal root profile, as required. At intermediate values of T_e (bold line), a topographic profile develops that retains the original scarp and develops an elevated bench below it.

Figure 3C shows the surface elastic stresses that result from the subsurface load shown in Figure 3A for the same three values of T_e . The stress profiles are not greatly affected by the variation in T_e , though high rigidities result in broader peaks and lower stress magnitudes. As Figure 2A predicts, surface stresses are primarily compressional on the thick-crust side and extensional on the thin-crust side. The peak surface stresses, 60–80 MPa, correspond to elastic strains of 0.06%–0.08%.

COMPARISON WITH OBSERVATIONS

Several broad aspects of the model results of Figure 3 resemble the observations summarized in Figure 1B. First, the topographic profiles are similar: e.g., the model develops an elevated bench below the scarp, similar to the observed transition zone. More important, the predicted zones of surface extension and compression closely mimic those actually observed: extension is predicted across the scarp and into the bench, whereas compression is predicted mainly south of the scarp. Although secondary compression is predicted in the lowlands (Fig. 3C), any such compressional features may well have been buried by the later emplacement of the shallow northern plains (Head et al., 2002). Third, the peak predicted compressive strains are $\sim 0.1\%$, in relatively close agreement with the measured strains of $\sim 0.2\%$ (Watters and Robinson, 1999). Thus, the lower crustal flow model does a good job of matching the observations.

EROSION

In order to simulate erosion, the same initial surface topography (Fig. 3B) was adopted, and a diffusion equation applied with constant diffusivity (cf. Perron et al., 2003). This results in removal of material from the highlands, and symmetrical deposition in the low-

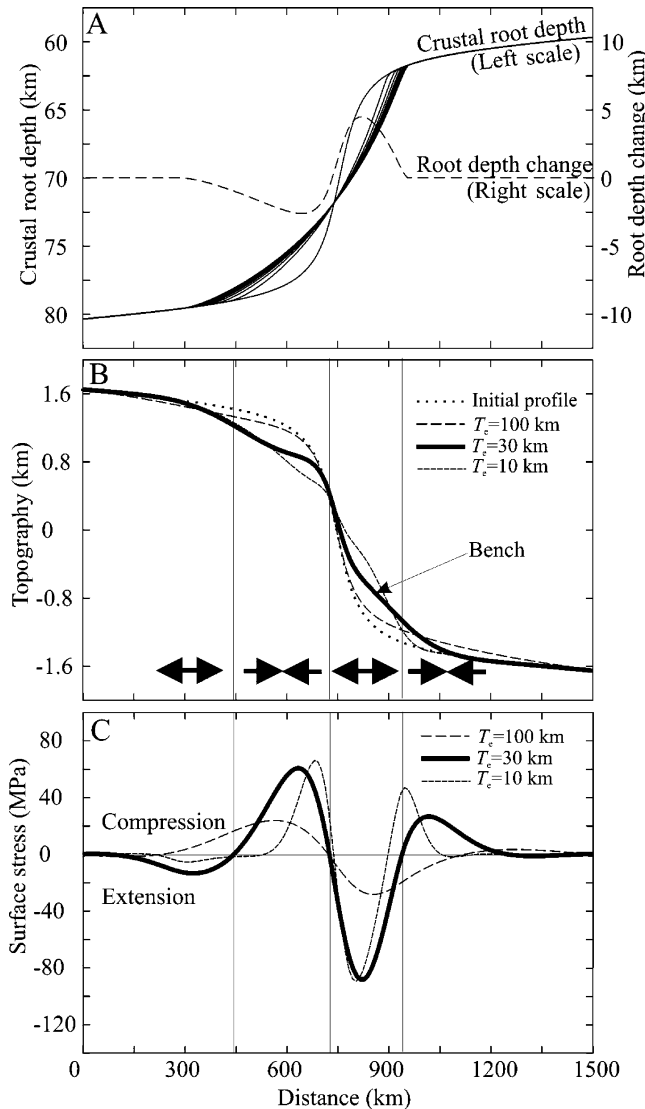


Figure 3. A: Evolution of depth to base of crust as result of lower crustal flow. Solid lines are plotted at 3 m.y. intervals for 100 m.y., using parameters given in text. Mean crustal thickness is 70 km, dry diabase rheology. Dashed line gives change in crustal root thickness. B: Surface topography resulting from change in crustal root thickness shown in A, calculated using equation 1. Dotted line is initial topography; other lines are final topography, dependent on elastic thickness T_e . Arrows denote regions of compression and extension deduced from stresses shown in C for $T_e = 30$ km. C: Stresses resulting from deflections obtained in B, calculated using equation 2. Vertical lines define regions of compression and extension for $T_e = 30$ km.

lands. The model was terminated when the peak thickness of material removed reached 0.45 km.

The removal of material from the highlands results in an upward load. The upward deflection in response to this load is calculated in a manner entirely analogous to equation 1, and the results are shown in Figure 4A. For a low elastic thickness, the upward deflection is essentially identical to the case of isostatic rebound and results in little net change in topography. For a high elastic thickness, little deflection occurs, the topographic change is correspondingly larger, and the stresses are reduced.

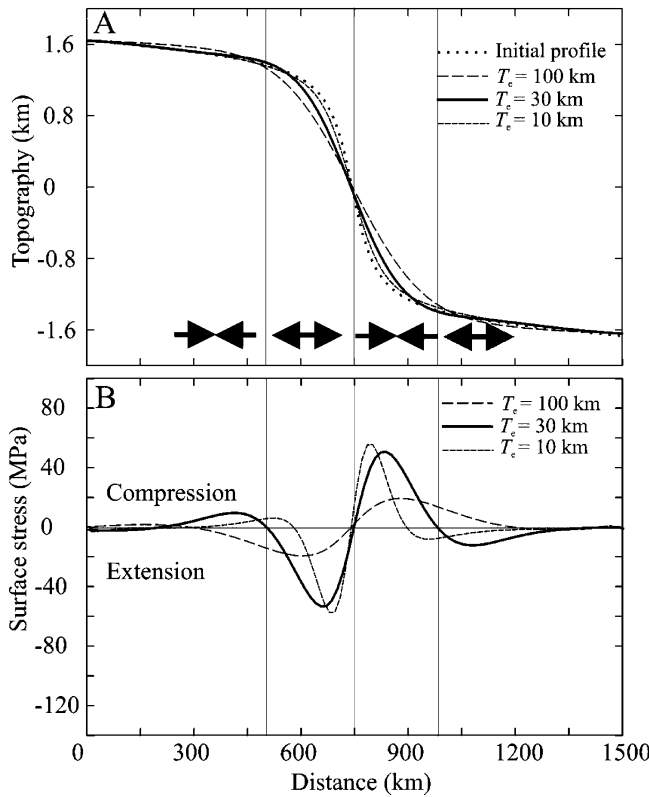
The surface stresses resulting from Figure 4A are calculated using equation 2 and are shown in Figure 4B. Although comparable in magnitude to the stresses shown in Figure 3C, the polarity is reversed, with stresses primarily compressional on the highland side and extensional on the lowland side. This stress pattern is opposite to that observed and suggests that erosion is not responsible for the observed tectonic features.

DISCUSSION AND CONCLUSIONS

Although Figure 3 depicts results for only one set of parameters, consideration of Figure 2 suggests that similar stress patterns will result, irrespective of the parameters, as long as moderate lower-crustal flow occurs. For example, increasing the initial heat flux by 30% and reducing the mean crustal thickness to 55 km results in a similar amount of crustal flow and an essentially identical stress pattern. Even larger heat fluxes or a significantly weaker rheology are likely to result in complete removal of the dichotomy topography. Conversely, to generate the stresses required to cause fault motion, some flow is required. For the case shown in Figure 3A, a T_e in the range of 1–70 km generates peak compressional stresses >40 MPa. Smaller or larger T_e values result in stresses that may be too small to generate fault motion. Whereas effects such as yielding and time-variable T_e are neglected here, they are unlikely to produce qualitatively different results.

Figure 3A suggests that most deformation happens early, whereas the observed tectonic

Figure 4. A: Topography following surface erosion. Dotted line gives initial topographic profile; material is then redistributed, using diffusion equation, until maximum amount of material removed is 0.45 km. Product of diffusivity and total time elapsed is 9000 km². Resulting load is converted into deflection using equation 1. Solid and dashed lines show resulting topography after this deflection occurs, for differing elastic thicknesses T_e . Arrows depict regions of compression and extension deduced from B for $T_e = 30$ km, as for Figure 3C.



features may be several hundred million years younger than the dichotomy. However, the model assumes that surface heat flux declines monotonically, which is not necessarily the case. For example, a putative early Hesperian thermal event associated with northern plains resurfacing (Head et al., 2002) would also generate an episode of enhanced crustal flow.

If moderate lower-crustal flow has occurred, it is likely to generate a negative gravity anomaly ahead of the surface dichotomy boundary. Another test involves drainage patterns. Figure 3B suggests that local slopes change, and may even reverse, when lower-crustal flow occurs. Such changes in slope direction could be inferred by careful analysis of ancient drainage patterns (e.g., Hynek and Phillips, 2001).

This work concludes that erosion is not responsible for the tectonic patterns observed. However, the geological evidence for ~1 km of denudation in the highlands is strong (Cradock and Maxwell, 1993; Hynek and Phillips, 2001). There are two possible resolutions of this paradox. One is that denuded material is redeposited locally and thus involves no regional mass transfer. The second is that, by the time the erosion occurred, the elastic thickness was sufficiently large that the stresses generated were too small to produce fault motion (cf. Fig. 4B).

ACKNOWLEDGMENT

I thank Greg Neumann, Shijie Zhong, and Tom Watters for helpful comments.

REFERENCES CITED

- Bird, P., 1991, Lateral extrusion of lower crust from under high topography in the isostatic limit: *Journal of Geophysical Research*, v. 96, p. 10,275–10,286.
- Cradock, R.A., and Maxwell, T.A., 1993, Geomorphic evolution of the Martian highlands through ancient fluvial processes: *Journal of Geophysical Research*, v. 98, p. 3453–3468.
- Frey, H.V., 2004, Impact constraints on the age and origin of the crustal dichotomy on Mars, *in* Workshop on Martian Hemispheres: Houston, Texas, Lunar and Planetary Institute Contribution 1213, abs. 4012.
- Frey, H.V., and Schultz, R.A., 1988, Large impact basins and the mega-impact origin for the crustal dichotomy on Mars: *Geophysical Research Letters*, v. 15, p. 229–232.
- Frey, H.V., Roark, J.H., Shockey, K.M., Frey, E.L., and Sakimoto, S.E.H., 2002, Ancient lowlands on Mars: *Geophysical Research Letters*, v. 29, 1384.
- Head, J.W., Kreslavsky, M.A., and Pratt, S., 2002, Northern lowlands of Mars: Evidence for widespread flooding and tectonic deformation in the Hesperian period: *Journal of Geophysical Research*, v. 107, doi: 10.1029/2000JE001445.
- Hynek, B.M., and Phillips, R.J., 2001, Evidence for extensive denudation of the Martian highlands: *Geology*, v. 29, p. 407–410.
- Irwin, R.P., Watters, T.R., Howard, A.D., and Zimbelman, J.R., 2004, Sedimentary resurfacing and fretted terrain development along the crustal dichotomy boundary, Aeolis Mensae, Mars: *Journal of Geophysical Research*, v. 109, E09011.
- Mackwell, S.J., Zimmerman, M.E., and Kohlstedt, D.L., 1998, High-temperature deformation of dry diabase with application to tectonics on Venus: *Journal of Geophysical Research*, v. 103, p. 975–984.
- McGill, G.E., and Dimitriou, A.M., 1990, Origin of the Martian global dichotomy by crustal thinning in the Late Noachian or Early Hesperian: *Journal of Geophysical Research*, v. 95, p. 12,595–12,605.
- McGill, G.E., Smrekar, S.E., Dimitriou, A.M., and Raymond, C.A., 2004, Crustal evolution of the Protonilus Mensae area, Mars, *in* Workshop on Mar-

- tian Hemispheres: Houston, Texas, Lunar and Planetary Institute Contribution 1213, abs. 4003.
- McGovern, P.J., Solomon, S.C., Smith, D.E., Zuber, M.T., Simons, M., Wiczorek, M.A., Phillips, R.J., Neumann, G.A., Aharonson, O., and Head, J.W., 2002, Localized gravity/topography admittance and correlation spectra on Mars: Implications for regional and global evolution: *Journal of Geophysical Research—Planets*, v. 107, 5136.
- McKenzie, D., Barnett, D.N., and Yuan, D.N., 2002, The relationship between Martian gravity and topography: *Earth and Planetary Science Letters*, v. 195, p. 1–16.
- Nimmo, F., 2002, Admittance estimates of mean crustal thickness and density at the Martian hemispheric dichotomy: *Journal of Geophysical Research—Planets*, v. 107, 5117.
- Nimmo, F., and Stevenson, D.J., 2001, Estimates of Martian crustal thickness from viscous relaxation of topography: *Journal of Geophysical Research*, v. 106, p. 5085–5098.
- Perron, J.T., Dietrich, W.E., Howard, A.D., McKean, J.A., and Pettegaa, J.R., 2003, Ice-driven creep on Martian debris slopes: *Geophysical Research Letters*, v. 30, 1747.
- Schultz-Ela, D.D., and Walsh, P., 2002, Modeling of grabens extending above evaporites in Canyonlands National Park, Utah: *Journal of Structural Geology*, v. 24, p. 247–275.
- Tanaka, K.L., 2004, Topographic and geomorphic modification history of the highland/lowland dichotomy boundary of Mars: 1. Noachian period, *in* Workshop on Martian Hemispheres: Houston, Texas, Lunar and Planetary Institute Contribution 1213, abs. 4023.
- Tanaka, K.L., Skinner, J.A., Hare, T.M., Joyal, T., and Wenker, A., 2003, Resurfacing history of the northern plains of Mars based on geologic mapping of Mars Global Surveyor data: *Journal of Geophysical Research—Planets*, v. 108, 8043.
- Turcotte, D.L., and Schubert, G., 2002, *Geodynamics*: New York, Cambridge University Press, 456 p.
- Wanke, H., and Dreibus, G., 1988, Chemical composition and accretion history of terrestrial planets: *Royal Society of London Philosophical Transactions, ser. A, Mathematical and Physical Sciences*, v. 235, p. 545–557.
- Watters, T.R., 2003a, Lithospheric flexure and the origin of the dichotomy boundary on Mars: *Geology*, v. 31, p. 271–274.
- Watters, T.R., 2003b, Thrust faults along the dichotomy boundary in the eastern hemisphere of Mars: *Journal of Geophysical Research*, v. 108, 5054.
- Watters, T.R., and Robinson, M.S., 1999, Lobate scarps and the Martian crustal dichotomy: *Journal of Geophysical Research—Planets*, v. 104, p. 18,981–18,990.
- Zhong, S.J., 1997, Dynamics of crustal compensation and its influences on crustal isostasy: *Journal of Geophysical Research*, v. 102, p. 15,287–15,299.
- Zhong, S.J., and Zuber, M.T., 2000, Long-wavelength topographic relaxation for self-gravitating planets and implications for the time-dependent compensation of surface topography: *Journal of Geophysical Research*, v. 105, p. 4153–4164.
- Zhong, S.J., and Zuber, M.T., 2001, Degree-1 mantle convection and the crustal dichotomy on Mars: *Earth and Planetary Science Letters*, v. 189, p. 75–84.
- Zuber, M.T., Solomon, S.C., Phillips, R.J., Smith, D.E., Tyler, G.L., Aharonson, O., Balmirio, G., Banerdt, W.B., Head, J.W., Johnson, C.L., Lemoine, F.G., McGovern, P.J., Neumann, G.A., Rowlands, D.D., and Zhong, S.J., 2000, Internal structure and early thermal evolution of Mars from Mars Global Surveyor topography and gravity: *Science*, v. 287, p. 1788–1793.

Manuscript received 5 November 2004

Revised manuscript received 21 February 2005

Manuscript accepted 28 February 2005

Printed in USA